Research Article
Comparative Study of Influence of Anions on Microstructural Development and Sintering of Nanosized Alumina

[1]Fadia Shaheen, [2]Tayyaba Ahmad, [3]Muhammad Irfan, [1]Bakht Bahadur Rana and [1]Rashad Mahmood
[1]Glass and Ceramic Research Centre, PCSIR Laboratories Complex, Lahore, 54000,
[2]Applied Chemistry Research Centre, PCSIR Laboratories Complex, Lahore, 54000,
[3]PITMAEM, PCSIR Laboratories Complex, Lahore, 54000, Pakistan

Abstract: Nanosized alumina has been synthesized by employing two aluminum salts with monovalent anions that are aluminum nitrate and aluminum chloride as precursors under identical reaction conditions by homogeneous precipitation method. In both the cases, gelation of aluminum hydroxide occurred in comparable pH regime and produced alumina nanoparticles with comparable average particle size, however, their sintering behavior and microstructure of finished products were not comparable. Nanopowders obtained from aluminum nitrate were highly consolidable and sinterable producing reasonable final densities conversely to nanopowders obtained from aluminum chloride which were less consolidable and sinterable, besides the final products showed microstructural flaws including cracks and outgrowths due to inherent passive thermal transformations of nanopowders and unavoidable interferences. DSC/TG, TDA, SEM-EDS, XRD techniques were employed to characterize the nanopowders and dense products.

Keywords: Aluminum chloride, aluminum nitrate, densification defects, nanoalumina precursors, sintering

INTRODUCTION

Nanosized alumina is quintessential ceramic material showing high strength, melting temperature, abrasion resistance, optical transparency and electric resistivity. More recent applications of nanosized alumina include catalyst substrates, the tube of Arc lamps and laser hosts. Possible new uses of nanoalumina are in electronic circuits, optical components, alumina fibers for composite and biomaterials. Traditional uses of alumina are furnace machinery, cutting tools, bearings and gem stones (Shackelford and Doremus, 2008).

Ceramic processing to produce ceramic parts with desirable properties is critical to the intrinsic properties of ceramic powders. These include average particle size, particle size distribution, shape, surface area and impurities. Besides the method of synthesis of ceramic powders, their fabrication processing also influences the microstructural developments and process of densification.

There are three main routes to synthesize ceramic nanopowders i.e., gaseous, solid and liquid phase. Among these, solution technique is most common and diverse methods to produce nanopowders (Matijevic'

et al., 1964; Matijevic' and Stryker, 1966). In the homogeneous precipitation of nanoalumina powders, the influence of anions on the formation of aluminum hydroxide has been investigated by several authors (Nagai et al., 1991; De Hek et al., 1978; Stol et al., 1976; Unuma et al., 1998; Ramanathan et al., 1996). During formation of aluminum hydroxide pH affects critically the crystallinity and morphologies of nanopowder as explained in our previous work (Shaheen et al., 2005, 2006). It has been reported that monovalent anions $NO3^{1-}$ and Cl^{1-} both get neutralized in comparable pH regime. It has also been quantified that at precipitation stage, the ratio of added $[OH]^{1-}/[Al]^{3+}$, in both the cases was more than 2.5 at pH value above 5 (Nagai et al., 1991; Vermeulen et al., 1975; Sato et al., 1980). The present study focuses on the relative effect of monovalent anions primarily on the sol-gel processing and particle profile of nanoalumina powders and subsequently on microstructural developments while densifying into final sintered alumina products.

In the present study, alumina nanopowders were produced from aluminum nitrate and aluminum chloride under identical reaction conditions to explore relative effect of monovalent anions

Corresponding Author: Dr. Fadia Shaheen, GCRC, PCSIR Labs Complex, Lahore Pakistan, Tel.: 0092 99230688-95; Fax: 0092 42 99230704

Table 1: Molar compositions of aluminum salt and urea

Sr. No	Composition symbol	Salt: Urea molar ratio	Aluminum Salt M/3l	Urea M/3l
1.	AN3 AC3	1:3	0.3	0.9
	AN5 AC5	1:5	0.3	1.5
2.		1:7	0.3	2.1
	AN7 AC7			
		1:9	0.3	2.7
	AN9 AC9			

Table 2: Parameters of cold compaction

Sr. No.	Composition	Pre-sintering Temp/Time (°C/hour)	Binder (2%)	Pressure (MPa)	Time (seconds)
1	AN	800/2	PVA	100	3
2	AC	800/2	PVA	100	3

MATERIALS AND METHODS

Aluminum nitrate nonahydrate $Al(NO_3)_3.9H_2O$ (Fluka) and aluminum chloride hexahydrate $AlCl_3.6H_2O$ (Fluka) were used as starting materials. Molar ratios of aluminum salts and urea $(NH_2)_2CO$ (Merck) are given in Table 1.

The sols were heated at 90°C temperature with constant stirring and volume was maintained to 6 L by adding distilled water. The pH of the sols has been monitored throughout the reaction at definite intervals of time. When pH value reached 7, the reaction was stopped.

Gels were washed several times using distilled water. A tray type freeze drier of Max series was used to sublime gels at -40°C. Nanopowders collected from freeze drier were consolidated into green bodies. After pre-sintering at 800°C for 2 h, the powders were damped with 2wt% (related to Al_2O_3) polyvinyl alcohol PVA (Hoechst, Frankfurt) and uniaxially pressed into 1X0.3" disks. The prerequisites and parameters of cold compaction are given in Table 2.

The green machined compacts were initially dried overnight at room temperature, heated at 100°C for 1 h in the electric oven and finally thermolysed at 800°C for 1 h. The digital electric laboratory oven WE 500HA and high temperature rapid heating electric furnace RHF/3 Carbolite, UK were used. Sintering was carried out up to 1400°C at the heating rate 5°C per minute and soaking time 3 h.

For TDA, specimens with 50 mm length and 20 mm width were fired up to 1600°C @ 20°C per minute in Horizontal Orton Dilatometer DIL 2016 STD.

X-ray diffraction measurements were conducted on Siemen's Diffractometer D5000. X-ray tube operated at 40 kV and 30 mA. Data was collected with a scintillation counter in the 10-70° range with a step of 0.05° and a counting time of 60 s/step.
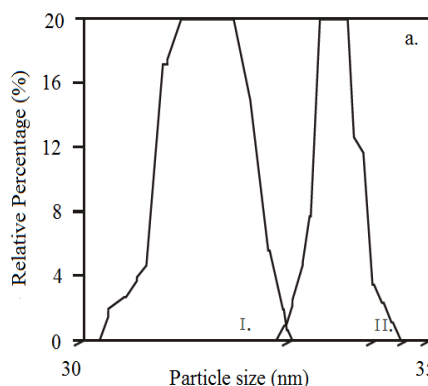

Fig. 1a: Average particle size distribution of I). AN nanopowders and II). AC nanopowders
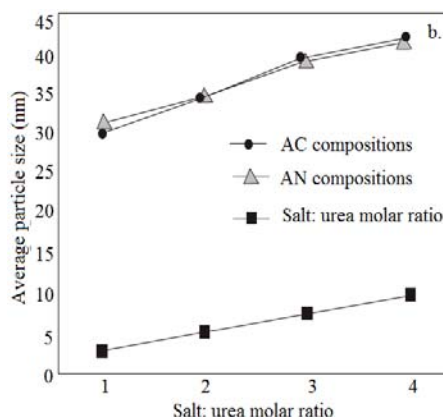

Fig. 1b: Change in average particle size as a function of salt: Urea molar ratio

A Hitachi S-3700, Japan SEM equipped with EDS, was used to acquire the image at the accelerating voltage 25 kV, working distance 5 mm and tilt angle 0°. To improve image resolution sample was coated with

platinum at 0.1 torr and 20 μA for 2 min which has been found optimum for a thin layer coating.

RESULTS AND DISCUSSION

Particle size analysis: Particle profile in Fig. 1a reveals that AN3 and AC3 are nanopowders having comparable average particle sizes, however; their particle size distribution was different.

AN3 has narrower while AC3 has relatively wider particle size distribution. Average particle size of both AN and AC compositions tend to increase as a function of the concentration of aluminum salt:urea molar ratio as depicted in Fig. 1b.

TDA Studies of AN compositions: The dilatometric curve of AN3 is presented in Fig. 2. Up to 800°C, the sample shows shrinkage in three steps; first percent linear change of 0.16% relates to the evolution of adsorbed water, second 0.58% to the dehydroxylation of pseudoboehmite and third 1.22% to the transformation into gamma alumina with the consequent peaks of shrinkage rate at 100, 231 and 325°C, respectively.

Beyond 800°C, linear shrinkage is 2.14% which depicts that densification begins at 895°C. Almost 80% of this shrinkage is complete up to 1100°C and the remaining 20% up to 1300°C. Two broad peaks associated with this shrinkage region appeared at 1020°C named T_1 and at 1098°C named as T_2. This compound peak shows the transformation from θ→α with c.c.p. to h.c.p. structural sequence.

The dilatometric results of AN5, AN7 and AN9 compositions are presented in Fig. 3. The general appearance of dilatometric curves of three specimens is same. However, linear shrinkage curves onset at 895, 899, 905 and 911°C, respectively. T_1 and T_2 peaks are ultimately shifted to higher temperatures by few

Fig. 3: Dilatometric curve of; (a): AN5 composition; (b): AN7 composition and; (c): AN9 composition

Fig. 4: Dilatometric curve of AC3 composition

degrees. The first peak appeared at 1020, 1024, 1030 and 1036 and second at 1098, 1102, 1109 and 1116°C, respectively. Thus sinterability of AN nanopowders increases with decrease in average particle size and vice versa.

TDA Studies of AC compositions: TDA curve of AC3 in Fig. 4 shows that the percentage linear shrinkage due to dehydration is 0.16%, due to dehydroxylation is 0.62% and further due to transformation of pseudoboehmite into gamma alumina is 1.21%. The peaks of shrinkage rate representing these three stages appeared at 100, 300 and 380°C, respectively.

Percentage linear shrinkage from room temperature to 800°C is 1.99% and onwards up to 1400°C is 1.85%. Densification begins at 1052°C with corresponding shrinkage peak at 1107°C.

The densification behavior of rest of three AC compositions is shown in Fig. 5. The change in sintering temperature has not been found in uniform
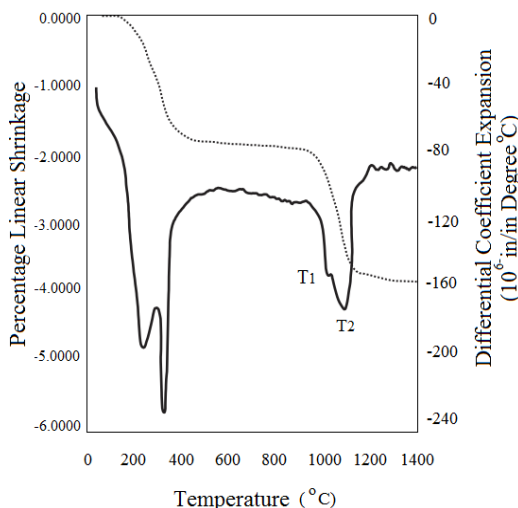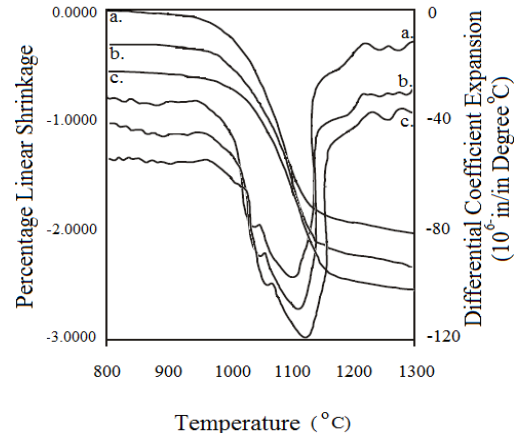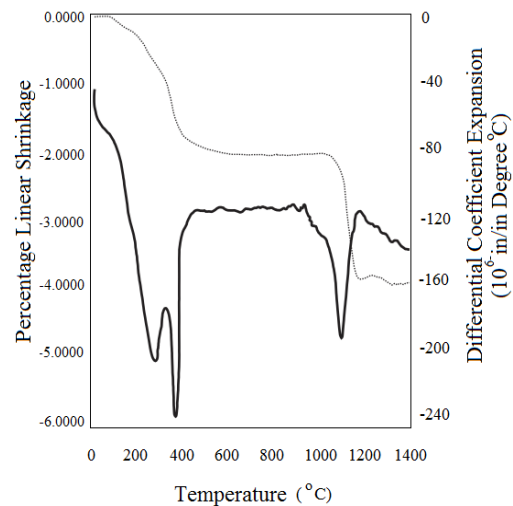
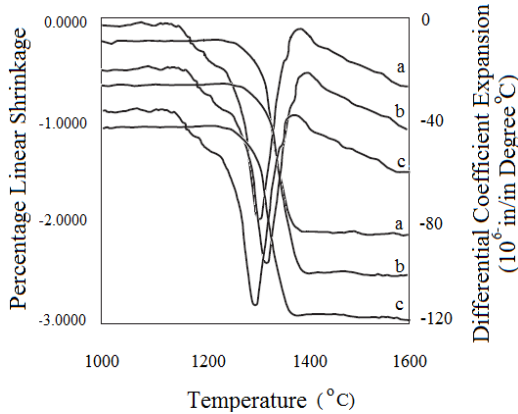Fig. 2: Dilatometric curve of AN3 composition

Fig. 5: Dilatometric curve of; (a): AC5 composition; (b): AC7 composition and; (c): AC9 composition

with the change in average particle size. AN and AC compositions showed different densification behavior in various aspects. Firstly, densification in ANs begins about 200° prior to ACs. Secondly, the rate peak is broad and compound in ANs whereas shingle and sharp in ACs. Thirdly, T_1 peak representing θ into α transformation appeared in ANs but not in ACs. Fourthly and finally, percentage linear shrinkage curve

in ACs conversely to ANs runs upward after 1200°C showing minor expansion.

SEM studies of AN compositions: AN compositions sintered at 1400°C are presented in Fig. 6a to 6d. The micrograph image ascertains that sintering is completed. The pores are closed intersecting at the grain boundaries. The grain size is isotropic with almost equiaxial grain shape and average size nearly 1micron. The sintering results show compliance with the dilatometric results.

SEM-EDS studies of AC compositions: AC compositions sintered at 1400°C are shown in Fig. 7a to 7d. During sintering two modes of damages were identified. One was cracks which appeared throughout the surface. These appeared due to incomplete pre-sintering of AC nanopowders. The green body prepared was defect free while on firing at 1100°C cracks appeared due to incomplete pre-sintering of powders.

Figure 8a shows green body and Fig. 8b shows cracks after firing 1100°C. AC3 powder pre-sintered at 800°C for 2 h in Fig. 9a shows pseudoboehmite bands along with theta and delta phase. This
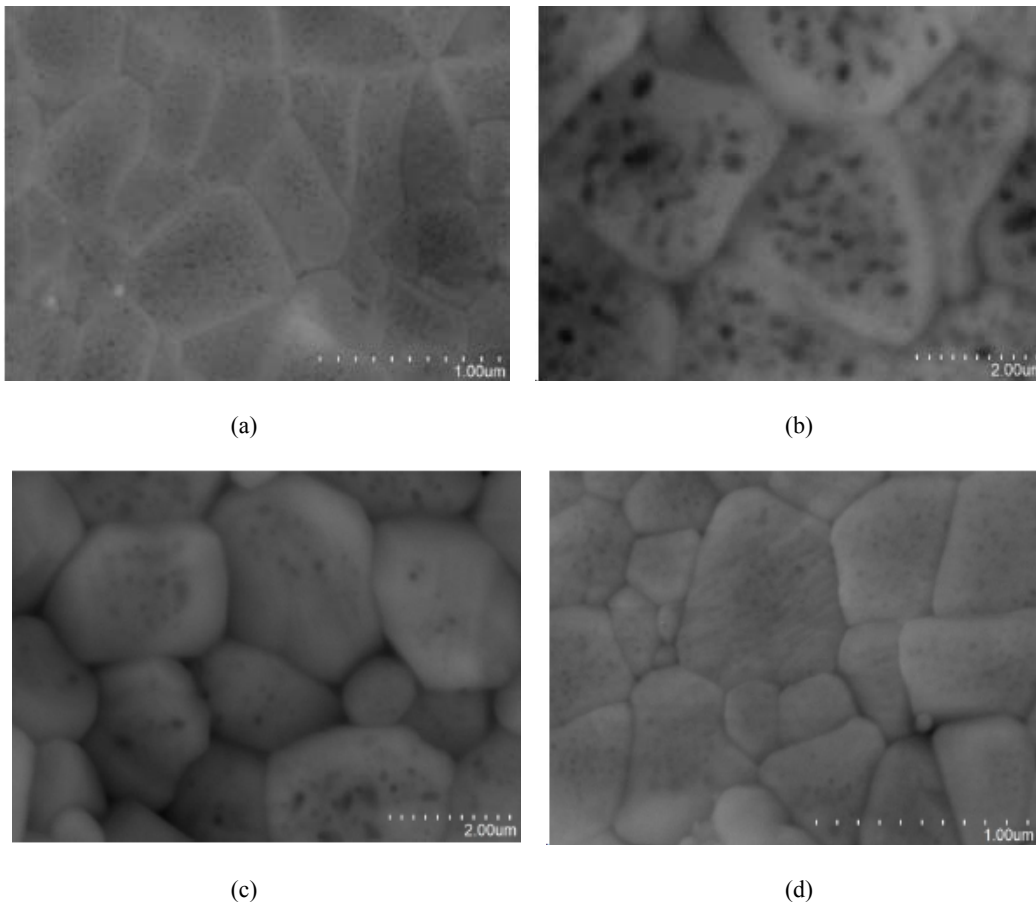

(a)

(b)

(c)

(d)

Fig. 6: SEM image of; (a): AN3; (b): AN5; (c): AN7 and; (d): AN9 sintered bodies
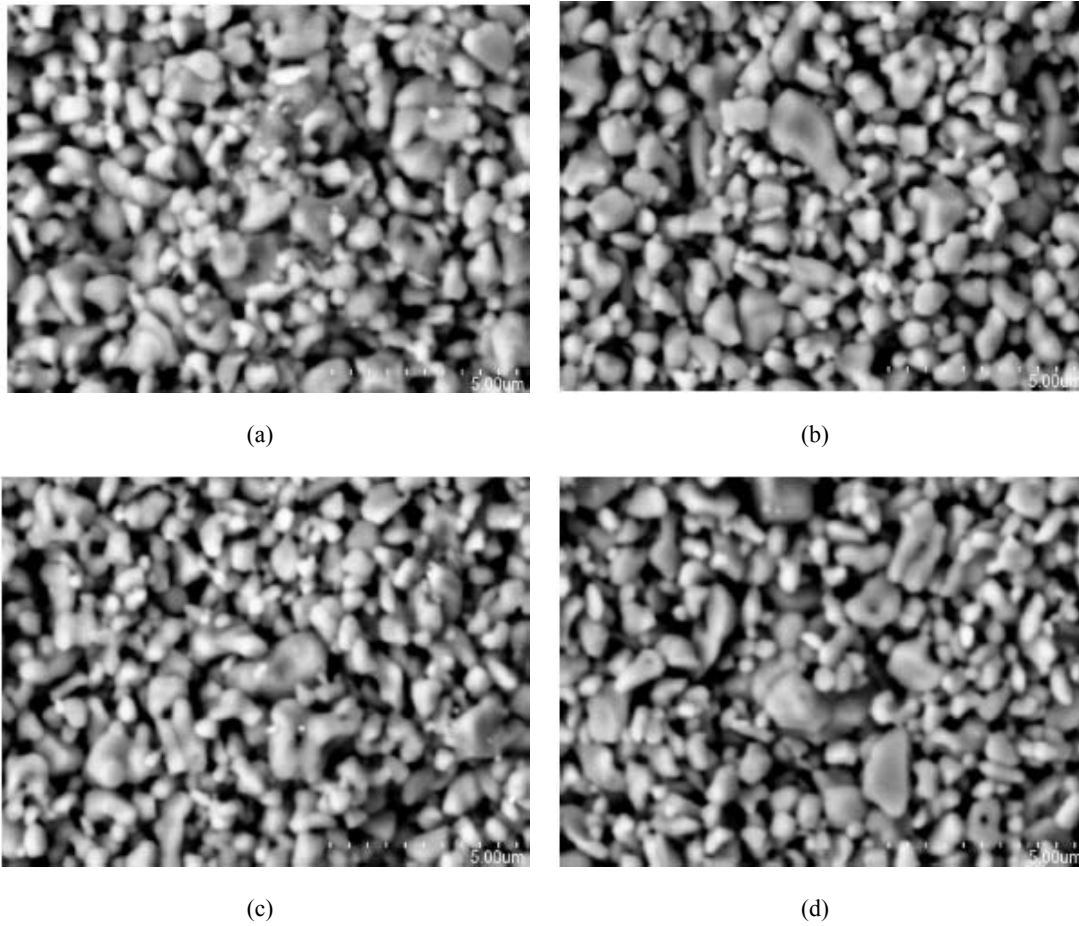
(a)

(b)

(c)

(d)

Fig. 7: SEM image of; (a): AC3; (b): AC5; (c): AC7 and; (d): AC9 sintered bodies
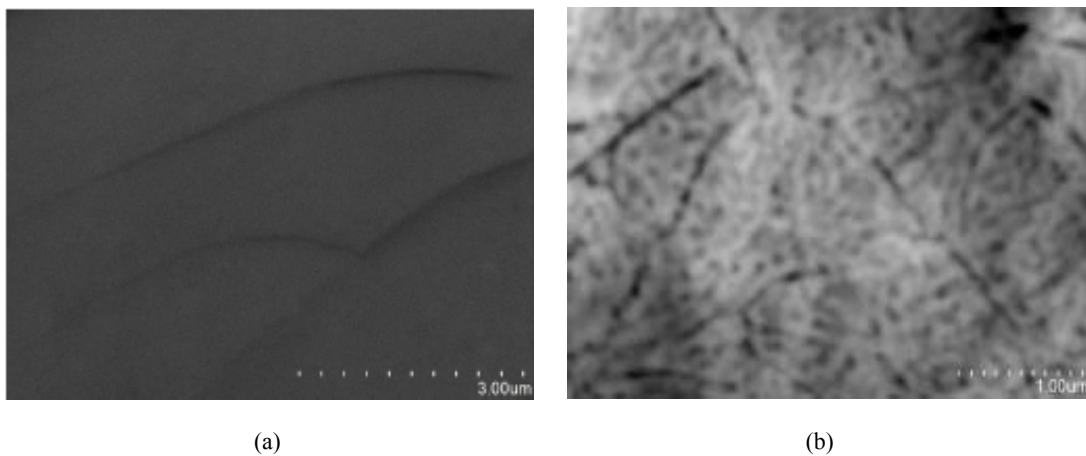

(a)

(b)

Fig. 8: SEM image of AC3 composition; (a): green body and; (b): fired at 1100°C

incompletely dehydroxylated pseudoboehmite produces internal gas pressures while sintering at elevated temperatures and causes cracks. On the contrary, the XRD graph of AN3 in Fig. 9b had no traces of pseudoboehmite showing that pre-sintering of powder is complete. Another mode of damage is due to impurities. SEM image and EDS graph are shown in Fig. 10a and 10b. The elements identified are aluminum, oxygen, chloride and traces of iron. Since the impurity emerged out randomly from the plane of the sample surface at frequent places so it seems that minor expansion in the dilatometry curve is related to it.
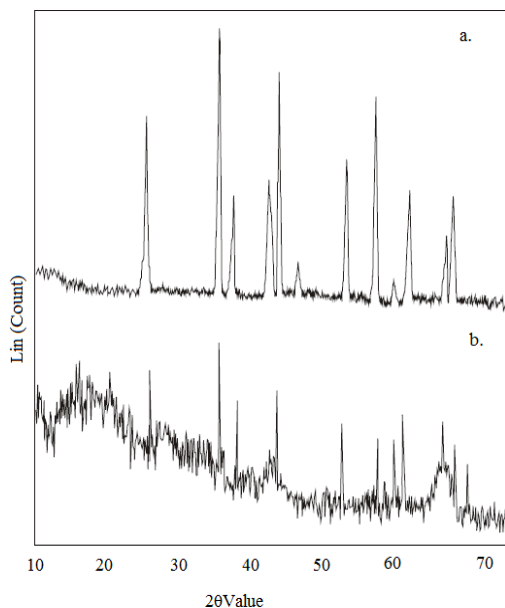
Fig. 9: XRD diffractogram of; (a): AN3 nanopower and; (b): AC3 nanopowder after firing at 800°C for 2 hr
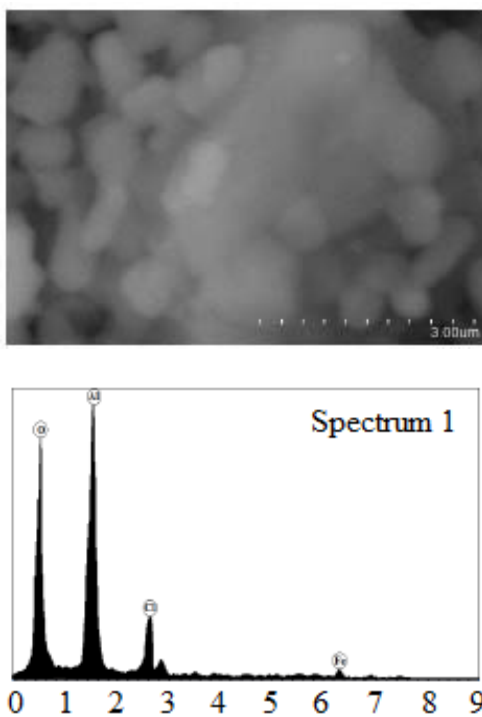

Fig. 10: SEM image and EDS spectrum of impurity orientation in AC3 composition

CONCLUSION

Aluminum nitrate-urea and aluminum chloride-urea were homogeneously precipitated under identical reaction conditions of concentration, dilution, gelating agent, temperature and stirring to produce alumina nanopowders. It was found that both the monovalent

anions NO_3^{1-} and Cl^{1-} initiated the gelatinous precipitation at comparable pH, the nanopowders so produced had the comparable average particle size, however, their relative pre- and post-sintering behavior was incomparable. Alumina nanopowders obtained from aluminum nitrate had higher sinterability as it began at about 200 degrees' lower temperature as compared to alumina powders obtained from aluminum chloride under identical fabrication conditions. In the presence of nitrate, final densities were reasonable and increase with the decrease in particle size whereas in the presence of chloride final densities are neither reliable nor sequential with the change in average particle size as shown in Fig. 10. Nanopowders produced from aluminum nitrate sintered to develop isotropic grain size with of 1micron with pores completely closed whereas, under identical sintering conditions, nanopowders produced from aluminum chloride exhibited two kinds of flaws. Firstly, cracks due to incomplete dehydroxylation of pseudoboehmite which in turn seems related to particle size distribution. Though average particle size in both the cases was same, however nanopowders from aluminum nitrate had the narrow range of particle size distribution as compared to nanopowders from aluminum chloride. Secondly and finally, is the outgrowth of impurities. The source of these two flaws is inherent and thus unavoidable as these appear in early stages and intensify with sintering.

REFERENCES

De Hek, H., R.J. Stol and P.L. De Bruyn, 1978. Hydrolysis-precipitation studies of aluminum (III) solutions. 3. The role of the sulfate ion. J. Colloid Interf. Sci., 64(1): 72-89.

Matijevic', E., G.E. Janauer and M. Kerker, 1964. Reversal of charge of lyophobic colloids by hydrolyzed metal ions. I. Aluminum nitrate. J. Colloid Sci., 19(4): 333-346.

Matijevic', E. and L.J. Stryker, 1966. Coagulation and reversal of charge of lyophobic colloids by hydrolyzed metal ions: III. Aluminum sulfate. J. Colloid Interf. Sci., 22(1): 68-77.

Nagai, H., S. Hokazono and A. Kato, 1991. Synthesis of aluminium hydroxide by a homogeneous Precipitation Method. I. Effect of additives on the morphology of aluminium hydroxide. Brit. Ceram. Trans., 90: 44-48.

Ramanathan, S., S.K. Roy, R. Bhat, D.D. Upadhaya and A.R. Biswas, 1996. Preparation and characterisation of boehmite precursor and sinterable alumina powder from aqueous aluminium chloride-urea reaction. J. Alloy. Compd., 243(1-2): 39-44.

Sato, T., S. Ikoma and F. Ozawa, 1980. Preparation of gelatinous aluminium hydroxide by urea from aqueous solutions containing chloride, nitrate and sulphate of aluminium. J. Chem. Technol. Biot., 30(1): 225-232.

Shackelford, J.F. and R.H. Doremus, 2008. Ceramic and Glass Materials: Structure, Properties and Processing. Springer, New York.

Shaheen, F., W.A. Shah, M.L. Mirza and M.P. Iqbal, 2005. Effect of concentration of $Al_2(SO_4)_3$ on the synthesis of Nanosized Alumina. J. Chem. Soc. Pak., 27(6): 602-605.

Shaheen, F., W.A. Shah, P.I. Qazi and M.L. Mirza, 2006. Development of nanoparticles of alumina by sol-gel method using inorganic Aluminum salts as precursors. Pak. J. Sci. Ind. Res., 49(2): 77-81.

Stol, R.J., A.K. Van Helden and P.L. De Bryun, 1976. Hydrolysis-precipitation studies of aluminum (III) solutions. 2. A kinetic study and model. J. Colloid Interf. Sci., 57(1): 115-131.

Unuma, H., S. Kato, T. Ota and M. Takahashi, 1998. Homogeneous precipitation of alumina precursors via enzymatic decomposition of urea. Adv. Powder Technol., 9(2): 181-190.

Vermeulen, A.C., J.W. Geus, R.J. Stol and P.L. De Bryun, 1975. Hydrolysis-precipitation studies of aluminum (III) solutions. I. Titration of acidified aluminum nitrate solutions. J. Colloid Interf. Sci., 51(3): 449-458.